Supplementary Information

DNAzyme-Augmented Bioorthogonal Catalysis System for Synergistic Cancer Therapy

*Yawen You,[a,b] Hao Liu, [a,b] Jiawei Zhu,[a,b] Yibo Wang, [c] Fang Pu, *, [a] Jinsong Ren, *, [a,b] and Xiaogang Qu*,[a,b]*

AUTHOR ADDRESS

[a] State Key Laboratory of Rare Earth Resources Utilization and Laboratory of Chemical Biology, Changchun Institute of Applied Chemistry, Chinese Academy of Sciences, Changchun 130022, P. R. China.

[b] University of Science and Technology of China, Hefei, Anhui 230029, P. R. China.

[c] Laboratory of Chemical Biology, Changchun Institute of Applied Chemistry, Chinese Academy of Sciences, Changchun 130022, P. R. China.

[*]Email: pufang@ciac.ac.cn, jren@ciac.ac.cn, xqu@ciac.ac.cn

Supplementary 1. General Information

Reagents and materials

Nanopure water (18.2 MΩ; Millpore Co., USA) was used in all experiments and to prepare all buffers. All oligonucleotides were purchased from Sangon Biotechnology Inc. (Shanghai, China) and used without further purification. The oligonucleotide sequences used in this work are listed in Table S1. The stock solutions of DNA were obtained by dissolving DNA in nanopure water. The reaction buffer contained 10 mM MOPS, 150 mM NaCl, pH 7.6. 3-(N-morpholino) propanesulfonic acid (MOPS), sodium ascorbate, Dichlorobis (triphenyl-phosphine) Palladium (II) (Pd (PPh3)2Cl2), ethynyltrimethylsilane (TMS), sodium azide (NaN3), phloroglucinol, iodocopper (CuI), 4-iodophenol and 4-dimethylaminopyridine (DMAP) were obtained from Alfa Aesar. Copper sulfate anhydrous ($CuSO_4$), phloroglucinol, dimethyl sulfoxide-D6, acetone-d6, Chloroform-D and dimethyl formamide (DMF) and hemin were obtained from Aladdin Reagent (Shanghai, China). Sodium chloride, sodium hydroxide (NaOH), dichloromethane (CH_2Cl_2), methyl alcohol (MeOH), $NaNO_2$, NaH_2PO_4, Na_2HP_4, anhydrous sodium acetate, acetic anhydride, ammonia water ($NH_3 \cdot H_2O$), conc. hydrochloric acid (conc. HCl) and conc. nitric acid (conc. HNO3) were purchased from Beijing Chemicals (Beijing, China). 3-(4, 5-dimethyl-2-yl)-2, 5-diphenyltetrazolium bromide (MTT) was from Sangon Biotechnology Inc. (Shanghai, P.R. China). 3,3′-dioctadecyloxacarbocyanine perchlorate (DiO-C1038) was from Beyotime Biotechnology. (Shanghai, P.R. China). Fetal bovine serum (FBS) was purchased from Zhejiang Tianhang Biotechnology Co., Ltd.

All other reagents were of analytical reagent grade and used as received.

Table S1. Oligonucleotides used in the study.

Name	Sequence (from 5' to 3')
WA-T30	TTTTTTTTTTTTTTTTTTTTTTTTTTTTTTCAACATCATCAACAC
AS1411-linker-T30	GGTGGTGGTGGTTGTGGTGGTGGTGGCAACATCATCAACACTTTTTTTTTTTTTTTTTTTTTTTTTTTTT

Note: The underlined parts are the sequences of AS1411 aptamer.

Measurements and characterizations

Transmission electron microscopic (TEM) images were captured by a FEI TECNAI G2 20 high-resolution transmission electron microscope operating at 200 kV. The zeta-potential of the nanoparticles was measured in a Zetasizer 3000HS analyzer. The DNA concentration was determined by measuring the absorbance at 260 nm at high temperature (90 ℃) by using a JASCOV-550 (JASCO International Co., LTD., Tokyo, Japan) spectrophotometer, equipped with a temperature-controlled cuvette holder controlled by using a circulating bath. Fluorescence spectra were detected by JASCO F-6000 fluorescence spectrometer with a Peltier temperature control accessory. ICP-MS measurements were performed on a TheroScientific Xseries II inductively coupled plasma mass spectrometer. The X-ray photoelectron Spectroscopy (XPS) spectra were analyzed by Thermo Fisher Scientific ESCALAB 250Xi Spectrometer Electron Spectroscopy (America). ^{1}H NMR spectra and ^{13}C NMR spectra were recorded on a Bruker-600 MHz NMR instrument. The High-Performance Liquid Chromatography (HPLC) was measured by Ultimate 3000. The Liquid Chromatography Mass Spectra (LC-MS) was obtained using Quattro Premier XE (America). The confocal laser scanning microscopy (CLSM) characterization was acquired by a (Nikon Eclipse Ni-E, Japan) top-of-the-line motorized upright. The flow cytometry data were obtained by BD LSRFortessa™ Cell Analyzer.

Supplementary 2. Preparation and Characterization of DNA-templated CuNPs

Preparation of DNA-templated Cu nanoparticles. DNA strands (1 μM) containing thymine-rich regions were dissolved in 3-(N-Morpholino) propanesulfonic acid (MOPS) buffer (10 mM, pH 7.6) and sodium ascorbate solution (2 mM). After blending completely, $CuSO_4$ solution (100 μM) was added and incubated for 15 min at room temperature. The mixtures were centrifuged via ultrafiltration centrifuge tube (retained molecular weight: 10K) to remove unreacted substance. Fluorescent copper nanoparticles were formed within 5 minutes (λex= 340 nm). The obtained G-quadruplex structure DNAzyme and DNA-templated CuNPs (G-Cu) were mixed with hemin (10 μM). After stirring about 3 hours, the G-Cu that loaded with hemin was formed (D-Cu).

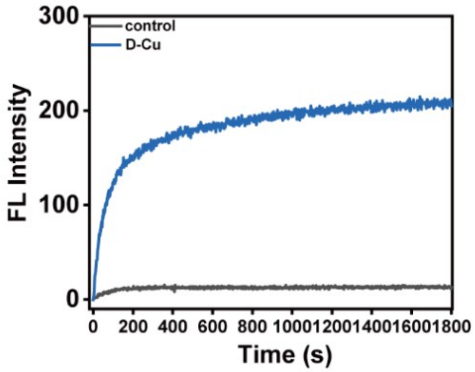

Figure S1. Real-time fluorescence intensity of D-Cu.

Table S2. The content of DNA-templated copper nanocatalysts.

	Catalyst	Cu (ppb)
1	D-Cu	4715
		4805
		4760
2	WA-Cu	4755
		4780
		4768

Note: In the catalytic study, the nanocatalysts with an equivalent amount of copper were tested.

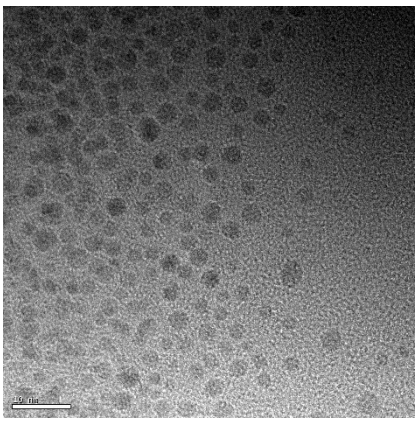

Figure S2. TEM image of D-Cu in DMEM with 10% FBS.

Peroxidase-like activity of D-Cu. The oxidation of TMB by D-Cu/H_2O_2 in 25 mM phosphate buffer (pH 4.0) produced a blue color with major absorbance peaks at 370 and 652 nm. Chemicals were added into 400 μL buffer solution in an order of certain amounts of the D-Cu, 5 μL TMB (final concentration 800 μM), and 40 μL H_2O_2 (final concentration 10 mM). In experiments, D-Cu was centrifuged to prevent the influence of the absorbance of D-Cu to the colorimetric reaction. Kinetic measurements were carried out by monitoring the absorbance change at 652 nm on a JASCO V550 UV-Vis spectrophotometer. Experiments were carried out using 10 μL D-Cu (final concentration 10 nM).

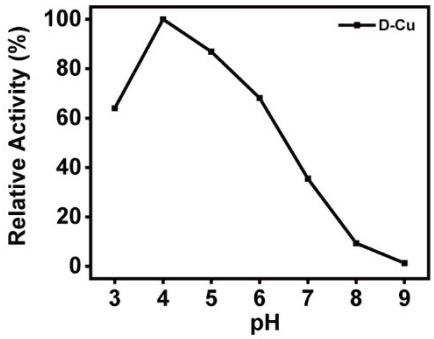

Figure S3. The influence of pH on peroxidase-mimicking activity of D-Cu. The solutions containing TMB (800 μM), H_2O_2 (10 mM), and D-Cu (10 nM) were prepared in phosphate buffer (25 mM) at different solution pH.

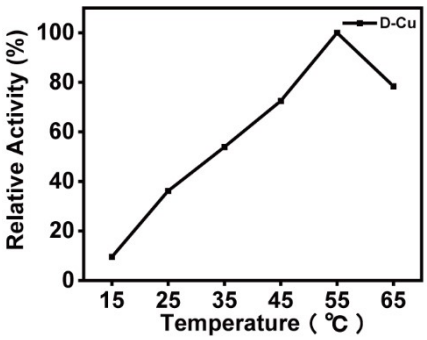

Figure S4. The influence of temperature on peroxidase-mimicking activity of D-Cu. The solutions containing TMB (800 μM), H_2O_2 (10 mM), and D-Cu (10 nM) were prepared in 25 mM phosphate buffer at pH 4.0.

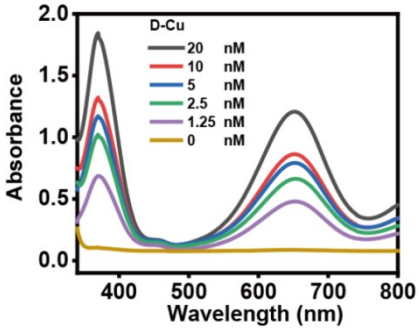

Figure S5. Impact of different D-Cu concentrations on TMB oxidization.The solutions containing TMB (800 μM), H_2O_2 (10 mM), and D-Cu of various concentrations were prepared with 25 mM phosphate buffer at pH 4.0.

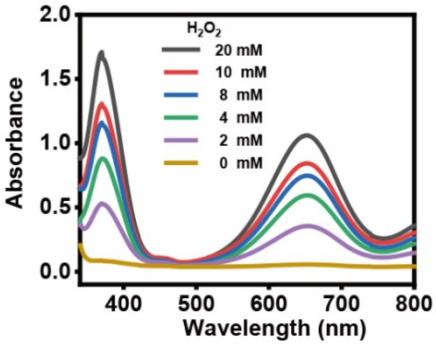

Figure S6. Impact of different H_2O_2 concentrations on TMB oxidization by the D-Cu. The solutions containing TMB (800 μM), D-Cu (10 nM), and H_2O_2 of various concentrations were prepared in 25 mM phosphate buffer at pH 4.0.

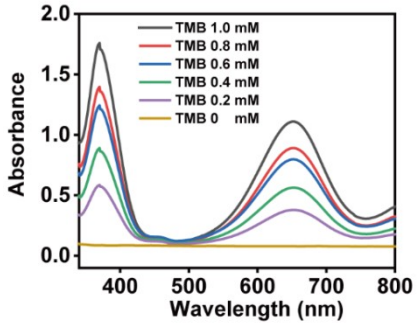

Figure S7. UV-vis absorption spectra of H_2O_2 treated with different concentration of TMB. The solutions containing H_2O_2 (10 mM), D-Cu (10 nM), and TMB of various concentrations were prepared in 25 mM phosphate buffer at pH 4.0.

Supplementary 3. D-Cu Promoted Click Reaction in vial

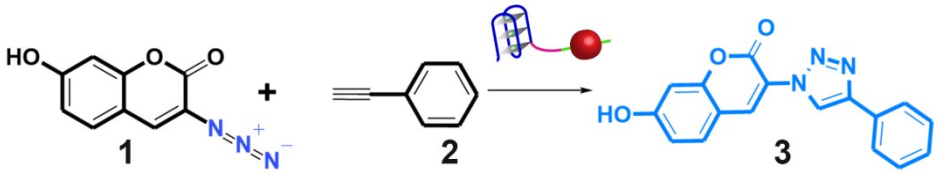

The click reaction between 3-azido-7-hydroxycoumarin, **1**, and phenylacetylene, **2** to form triazole **3** in vial, was carried out to assess the catalytic efficiency of D-Cu. Briefly, 5 µM D-Cu, 10 µM **1** (4 mM in DMSO) and **2** were mixed at 25℃ in water. D-Cu and D-Cu+H_2O_2 were incubated with **1** and **2** in vial, respectively. The mixture was instantaneously showed cyan-blue fluorescence, demonstrating the superior catalytic activity of the D-Cu in the presence of H_2O_2. The fluorescence of the mixture was detected via fluorescence spectrometer.

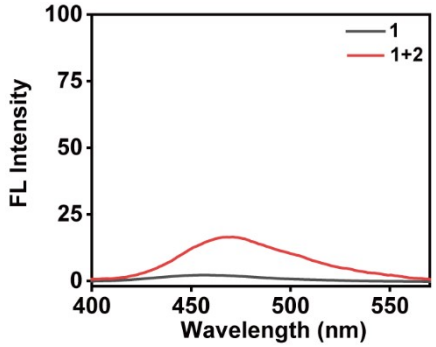

Figure S8. Fluorescence spectra of the precursors **1** and **2**.

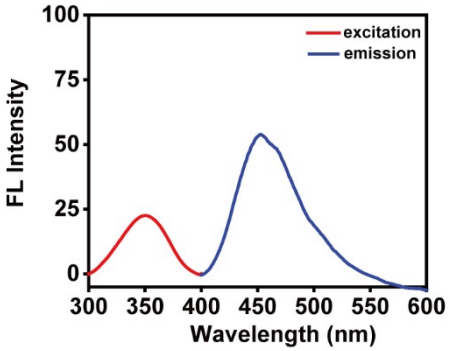

Figure S9. Excitation and emission spectra of **3** in H_2O. Cycloaddition of **1** and **2** afforded **3** (λ_{ex} =340 nm and λ_{em} =460 nm).

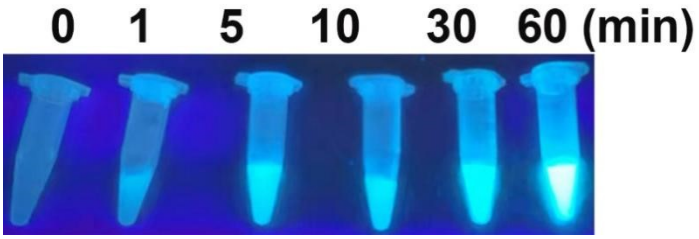

Figure S10. Fluorescence image of the CuAAC reaction in H_2O catalyzed by D-Cu+ H_2O_2 at different time (0, 1, 5, 10, 30, 60 min).

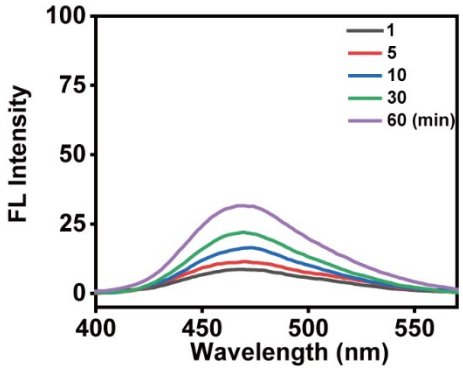

Figure S11. Fluorescent spectra of $CuSO_4$ catalyzed CuAAC reaction at different reaction time in vial. The experiment conditions of reactants: 5 μM $CuSO_4$, 25 μM sodium ascorbate, 10 μM **1** (4 mM in DMSO) and **2** were mixed at 25 ℃ in water.

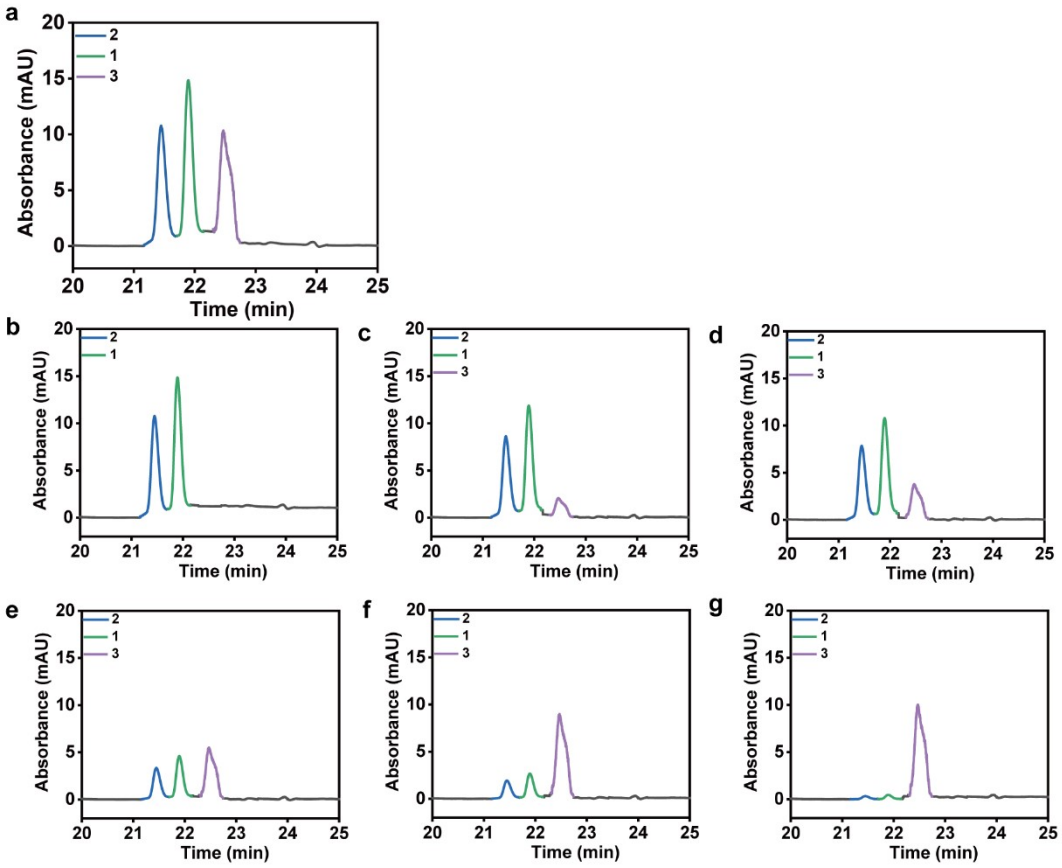

Figure S12. HPLC analysis of CuAAC reaction catalyzed by D-Cu in the presence of H_2O_2. a) HPLC chromatogram showing compound 2 at retention time 21.6 min, compound 1 at 22.2 min and product 3 at 22.5 min. b-g) HPLC chromatogram of catalytic reaction with **1** and **2** co-incubations at 0, 1, 5, 10, 30, 60 min with D-Cu in the presence of H_2O_2, respectively.

The analyses of high performance liquid chromatography (HPLC) conditions:

Detector: UV detector

Wavelength: 254 nm

Chromatographic column: Waters T3 C18 column (250×4.6mm, 5μm)

Mobile phase: A: methanol; B: 0.02mol/L Ammonium acetate solution (gradient elution)

Flow rate: 0.6 ml/min

Injection volume: 10 μL

Column temperature: 25 ℃

Table. The analyses of high performance liquid chromatography conditions

Time（min）	A phase concentration（%）	B phase concentration（%）
0	5	95
5	5	95
10	30	70
15	50	50
20	80	20
40	80	20
45	5	95
55	5	95

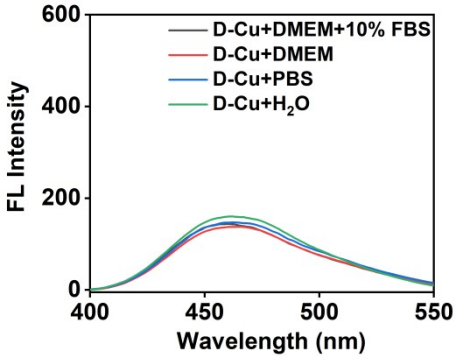

Figure S13. Fluorescence spectra of D-Cu- catalyzed CuAAC reaction in H_2O, PBS, DMEM and DMEM with 10% FBS. The experimental conditions of reactants: 5 μM D-Cu, 10 μM **1** (4 mM in DMSO) and **2** were mixed at 25 ℃ in water, PBS, DMEM and DMEM with 10% FBS, respectively.

***In silico* simulations**

The single-stranded DNA model was built manually based on the nucleic acid secondary structure prediction web server, RNAstructure 6.0.1[1]. The model was solvated in TIP3P water molecules and 150 mM KCl in a 98×98×98 $Å^3$ box. The system simulated by the NAMD2.12 package[2] with CHARMM C36 force field[3-4] to pursue a stable conformation. It was run at the temperature of 310.15 K and the pressure of 1 atm. The Nosé-Hoover Langevin piston method[5-6] was applied for the pressure control and the Langevin thermostat for the temperature coupling. The Particle Mesh Ewald algorithm was used to treat Long-range electrostatic

interactions[7]. 10-12 Å was employed to switch off the non-bonded interactions. The docking poses of ligands were determined by AutoDock Vina 1.1.2[8]. Optimal binding sites were searched in a box of 30 Å × 30 Å × 30 Å, in which the best poses were picked for further analysis. The other options of AutoDock Vina were set as default. The binding interactions between DNA and ligand was analyzed by LigPlot+[9].

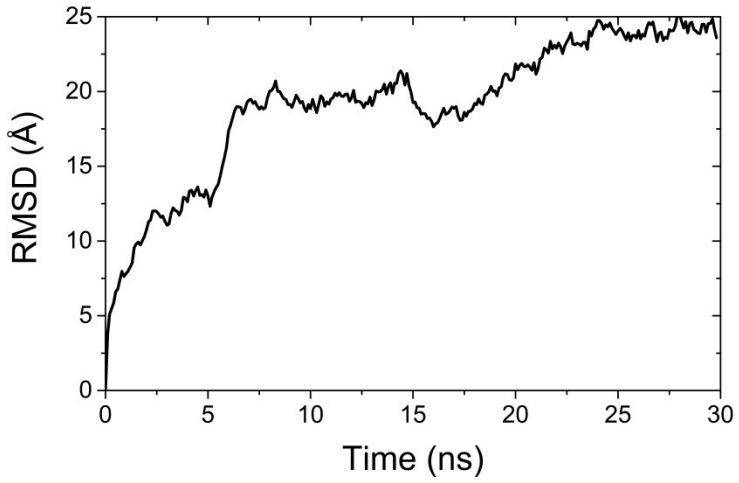

Figure S14. The molecular dynamics simulation of D-Cu structure. The time step was set as 2 fs and the system was run for 30 ns. The last frame of simulation was used for docking. The root-mean-square deviation (RMSD) values during the simulation indicated that the linker DNA and the AS1411 DNA can reach a stable state in 25 ns.

Table S3. The yields of different catalysts in CuAAC in H_2O.

Time(min) / Catalysts	1	5	10	30	60
0	**0.06**	**1.6**	**2.3**	**3.5**	**4.1**
$CuSO_4$+NaASC	**1.5**	**1.9**	**2.7**	**3.7**	**8.5**
D-Cu	**8.3**	**10.8**	**15.0**	**28.6**	**46.9**
D-Cu+H_2O_2	**18.9**	**35.7**	**56.7**	**90.1**	**>99**

First, **1** and **2** were co-incubated with H_2O, $CuSO_4$/NaASC, D-Cu, D-Cu in the presence of H_2O_2 for 0, 1, 5, 10, 30, 60 min, respectively. Then, the fluorescence intensity of triazole **3** produced by click reaction was tested to assess the catalytic efficiency via JASCO F-6000 fluorescence spectrometer. The results of

fluorescence spectra and high performance liquid chromatography (HPLC) presented that the catalytic transformation of D-Cu in the presence of H_2O_2 was almost completed within 60 min. According to the fluorescence analysis, the yields for different catalysts in CuAAC in H_2O were shown in Table S3.

Supplementary 4. Activating the Fluorescence Probe by D-Cu inside Cell

Cellular culture

The nucleolin-overexpressed cell line HeLa and the normal cell line HEK 293 were cultured with complete medium which was composed of high glucose DMEM, 10% FBS and 1% Penicillin-Streptomycin. The cells were placed in fresh medium every 3 days.

Cell viability assay

The cells with a density of 5000 cells/well were seeded in 96-well plate. After incubating for 24 h, the as-prepared D-Cu at indicated concentrations (0, 3.125, 6.25, 12.5, 25, 50 μM) were added, respectively. After culturing for another 24 h, cell medium was removed. And 100 μL of MTT solution was added to every well for additional 4 h. The medium of each well was replaced by 100 μL DMSO. The absorbance was measured by a Bio-Rad model-680 microplate reader at 570 nm. The cell viability was estimated according to the following equation: Cell Viability (%) = $(OD_{treated}/OD_{control}) \times 100\%$. $OD_{control}$ was obtained in the absence of nanocatalysts, whereas $OD_{treated}$ was obtained in the presence of nanocatalysts.

Cellular internalization of D-Cu and WA-Cu quantified by ICP-MS.

HeLa and HEK-293 cells were preincubated with D-Cu (5 μM) or WA-Cu (5 μM) for different time, then washed with PBS for 3 times. After the cells were digested by trypsin, lysis buffer (300 μL) was added. The obtained cell lysate was treated with mixture of HNO_3 and H_2O_2 (3:1 mL) overnight. Then aqua regia (3 mL) was added to the samples for another 2-3 h. The obtained samples were dried and re-dispersed into water, followed by analysis using ICP-MS.

Cellular internalization of D-Cu and WA-Cu quantified by Confocal microscopy images.

HeLa and HEK-293 cells were preincubated with D-Cu (5 μM) or WA-Cu (5 μM) for different time, then washed with PBS for 3 times. The fluorescence images were taken by OLYMPUS-BX51 microscopes with U-25ND25 filter.

Confocal microscopy imaging of D-Cu mediated click reactions in living cells. HeLa and HEK-293 cells were seeded on sterilized cover slips for 6 h in 24-well plates. D-Cu (5 μM), G-Cu (5 μM), WA-Cu (5 μM) was added and incubated with the cells for 4 h, respectively. Then the cells were washed with PBS for 3 times. Next, azide coumarin **1** (10 μM) and alkyne **2** (10 μM) were added and incubated with the cells for 12 h, followed by washing with PBS for 2 times. After staining cytomembrane by DiOC18(3), the fluorescence images were taken by OLYMPUS-BX51 microscopes with U-25ND25 filter.

Flow cytometric analysis of D-Cu mediated click reactions in living cells. HeLa and HEK-293 cells were seeded on sterilized cover slips for 6 h in 24-well plates. D-Cu (5 μM), G-Cu (5 μM), WA-Cu (5 μM) was added and incubated with the cells for 4 h, respectively. then washed with PBS for 3 times. Next, azide coumarin **1** (10 μM) and alkyne **2** (10 μM) were added and incubated with the cells for 12 h. After being washed with PBS for 2 times, the cells were harvested using trypsin and resuspended in PBS. The intracellular fluorescence of product **3** was analyzed using flow cytometry (450/50).

LC-MS analysis of D-Cu mediated click reactions in living cells. The HeLa cells were plated in 6-well plates for CuAAC reaction. D-Cu (5 μM) was incubated with HeLa cells for 4 h, then washed with PBS for 3 times. Then, azide coumarin **1** (10 μM) and alkyne **2** (10 μM) were added and incubated with the cells for 12 h. After the reaction was completed, the cells were treated with trypsin, collected in ultrapure water, and then lysed by sonication. The resulting lysate was centrifuged at 12470 g

for 5 min. The supernatant was extracted to mix with cold acetone and kept at -20°C overnight. Then the mixture was centrifuged at 12470 g for 15 min to collect the precipitate. The precipitate was re-dispersed in methanol and analyzed by LC-MS.

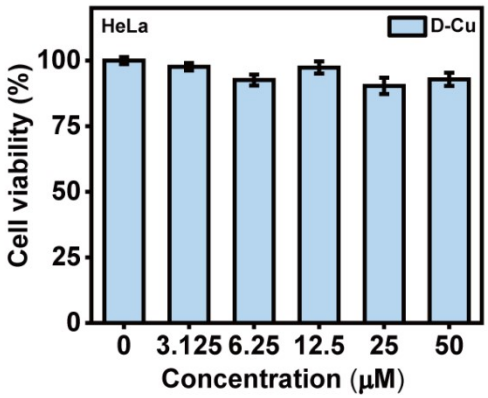

Figure S15. MTT assay of HeLa cells treated with different concentrations of D-Cu. Data were presented as mean ± SD (n = 3 independent experiments).

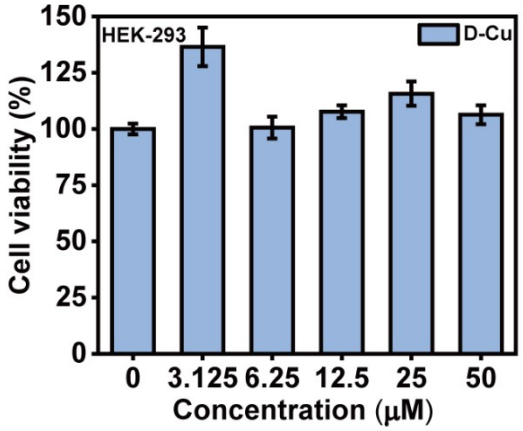

Figure S16. MTT assay of HEK-293 cells treated with different concentrations of D-Cu. Data were presented as mean ± SD (n = 3 independent experiments).

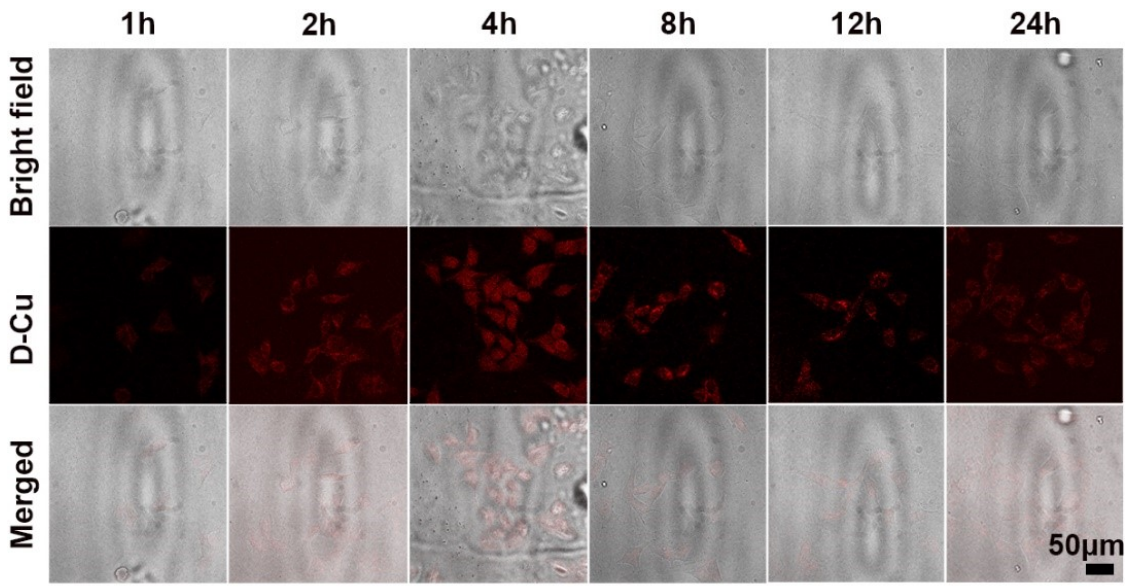

Figure S17. Confocal microscopy images for tracking the cellular internalization of D-Cu by HeLa cells at different time points (1, 2, 4, 8, 12 and 24 h, respectively). Images are representative of three independent biological samples. Scale bars: 50 μm.

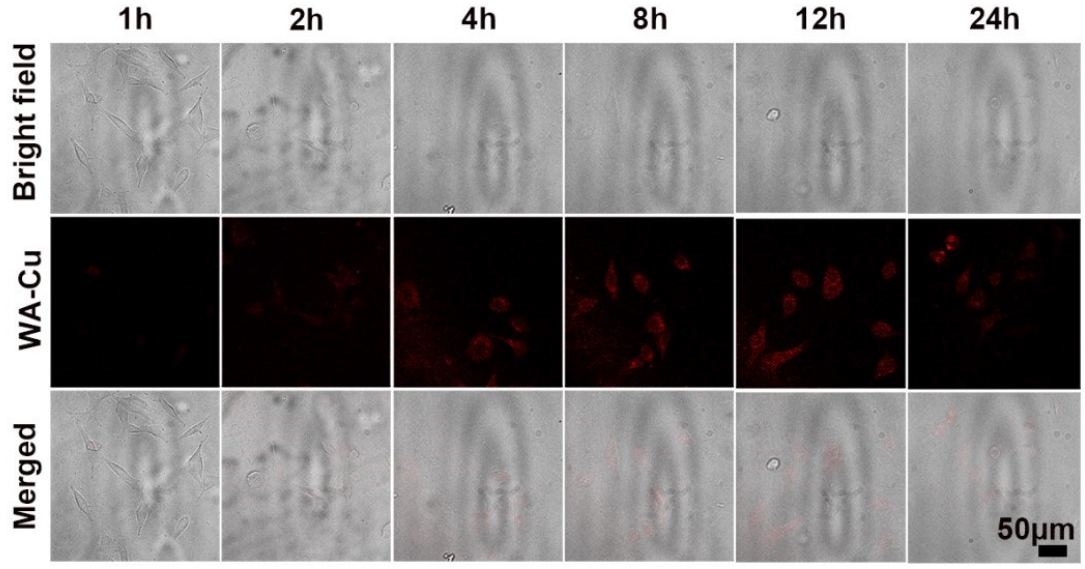

Figure S18. Confocal microscopy images for tracking the cellular internalization of WA-Cu by HeLa cells at different time points (1, 2, 4, 8, 12 and 24 h, respectively). Images are representative of three independent biological samples. Scale bars: 50 μm.

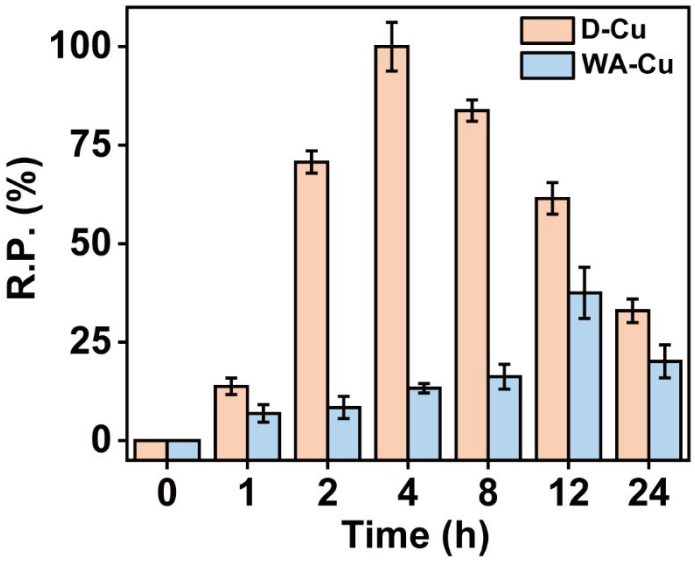

Figure S19. Cellular uptake of D-Cu and WA-Cu tracked by ICP-MS in 0, 1, 2, 4, 8,12 and 24 h. Data were presented as mean ± SD (n = 3 independent experiments).

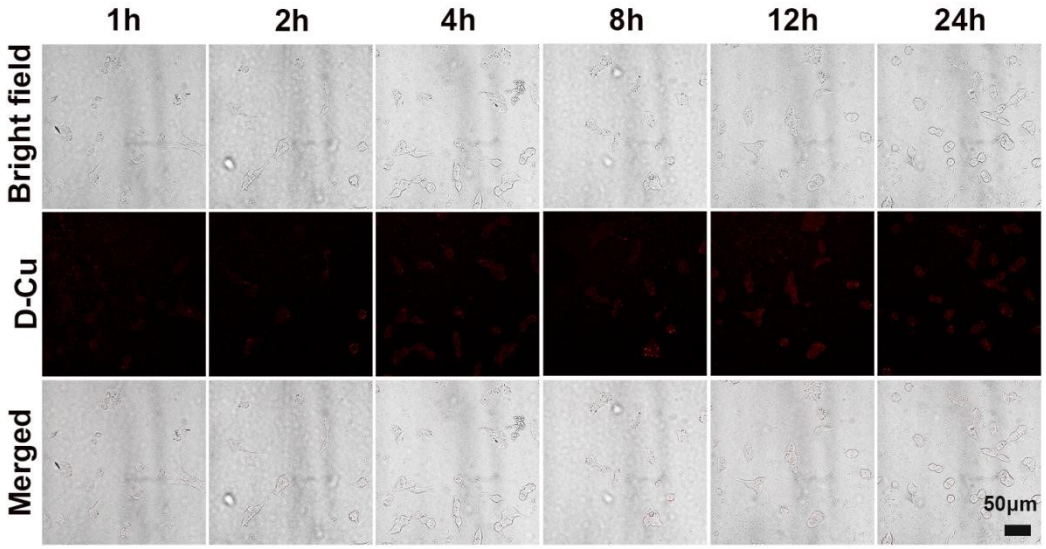

Figure S20. Confocal microscopy images for tracking the cellular internalization of D-Cu by HEK-293 cells at different time points (1, 2, 4, 8, 12 and 24 h, respectively). Images are representative of three independent biological samples. Scale bars: 50 μm.

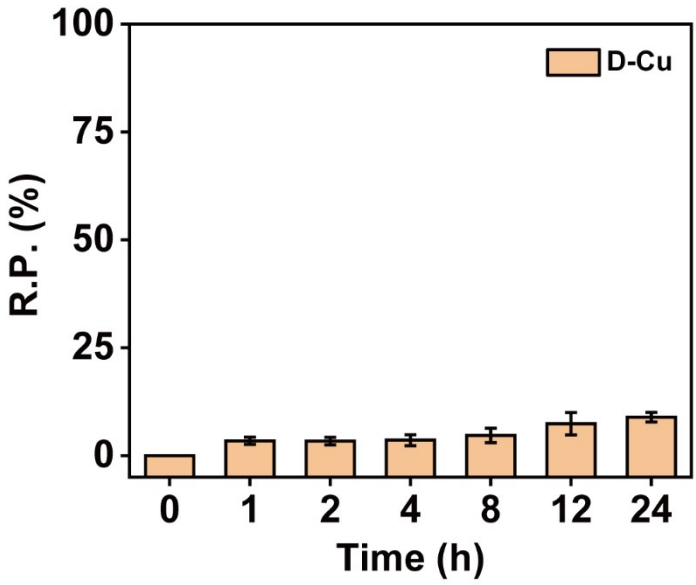

Figure S21. Uptake of D-Cu by HEK-293 cells tracked by ICP-MS in 0, 1, 2, 4, 8,12 and 24 h. Data were presented as mean ± SD (n = 3 independent experiments).

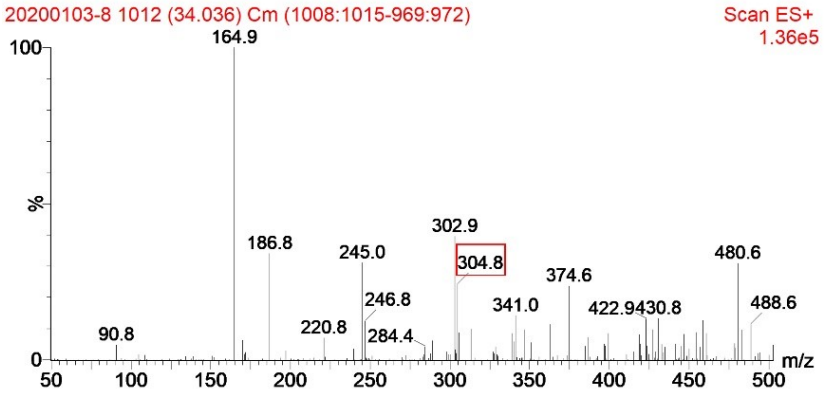

Figure S22. LC-MS analysis of the cell lysate to confirm the presence of click coupling product **3**.

Supplementary 5. Synthesis of Resveratrol Analogue Catalyzed by D-Cu in Living Cells.

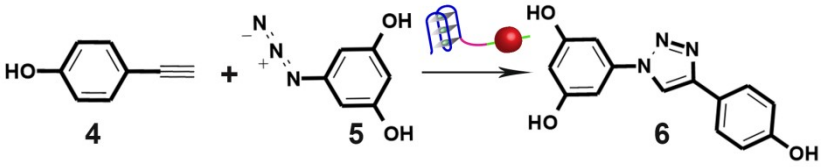

Determination of ROS Generation in vitro: For ROS detection, HeLa cells were randomly seeded in six-well plates in DMEM for 12 h before further manipulation. Then cells were incubated with G-Cu (5 μM), WA-Cu (5 μM) and D-Cu (5 μM) for 4 h. The treated cells were washed with PBS twice and incubated with 20 μM of prodrugs **4** and **5** for 12 h. Next, the treated cells were washed with PBS twice and incubated with 10 μM of DCFH-DA for 30 min. After the unloaded probe was removed with PBS, the fluorescence intensity of cells was monitored via confocal laser scanning microscope (CLSM).

Flow cytometric analysis. HeLa and HEK-293 cells were seeded on sterilized cover slips for 6 h in 24-well plates. D-Cu (5 μM), WA-Cu (5 μM) and G-Cu (5 μM) were added and incubated with the cells for 4 h, then washed with PBS for 3 times. Next, prodrug **4** (20 μM) and prodrug **5** (20 μM) were added and incubated with the cells for 12 h. After being washed with PBS for 2 times, the cells were harvested using trypsin and resuspended in PBS. The apoptosis of these cells induced by resveratrol analogue was analyzed by double staining with Annexin VFITC and propidium iodide using commercial apoptosis detection kit. The flow cytometry data were obtained by BD LSRFortessa™ Cell Analyzer and analyzed using FlowJo_V10. software.

LC-MS analysis of D-Cu mediated click reactions in living cells. The HeLa cells were plated in 6-well plates for CuAAC reaction. D-Cu (5 μM) was incubated with HeLa cells for 4 h, then washed with PBS for 3 times. Then, **4** (20 μM) and **5** (20 μM) were added and incubated with the cells for 12 h. After the reaction was completed,

the cells were treated with trypsin, collected in ultrapure water, and then lysed by sonication. The resulting lysate was centrifuged at 12470 g for 5 min. The supernatant was extracted to mix with cold acetone and kept at -20°C overnight. Then the mixture was centrifuged at 12470 g for 15 min to collect the precipitate. The precipitate was re-dispersed in methanol and analyzed by LC-MS.

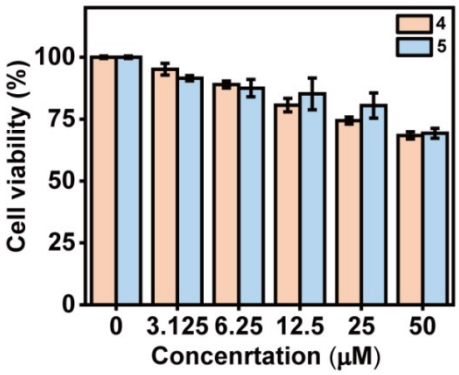

Figure S23. MTT assays of HeLa cells treated with different concentrations of **4** and **5**. Data were presented as mean ± SD (n = 3 independent experiments).

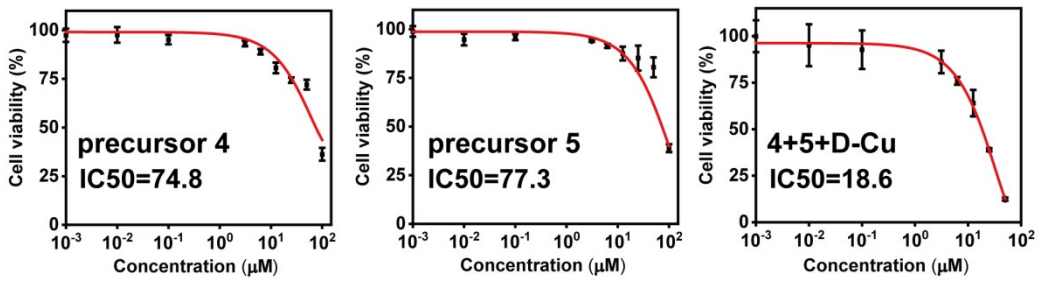

Figure S24. Cell viability assay of HeLa cells treated with the precursors **4**, **5**, and **4**+**5**+D-Cu with different concentrations, respectively. Data were presented as mean ± s.d. (n = 3).

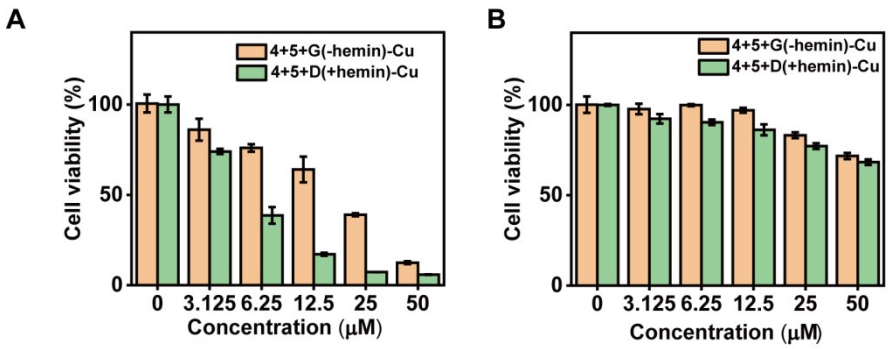

Figure S25. A) Cell viability of HeLa cells treated with **4**+**5**+G(-hemin)-Cu and **4**+**5**+D(+hemin)-Cu, respectively. B) Cell viability of HEK-293 cells treated with **4**+**5**+G(-hemin)-Cu and **4**+**5**+D(+hemin)-Cu, respectively.

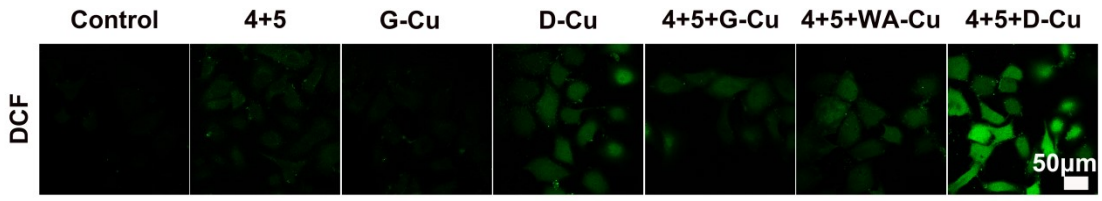

Figure S26. Confocal microscopy images for tracking the cellular internalization of D-Cu by HeLa cells. Scale bars, 50 μm.

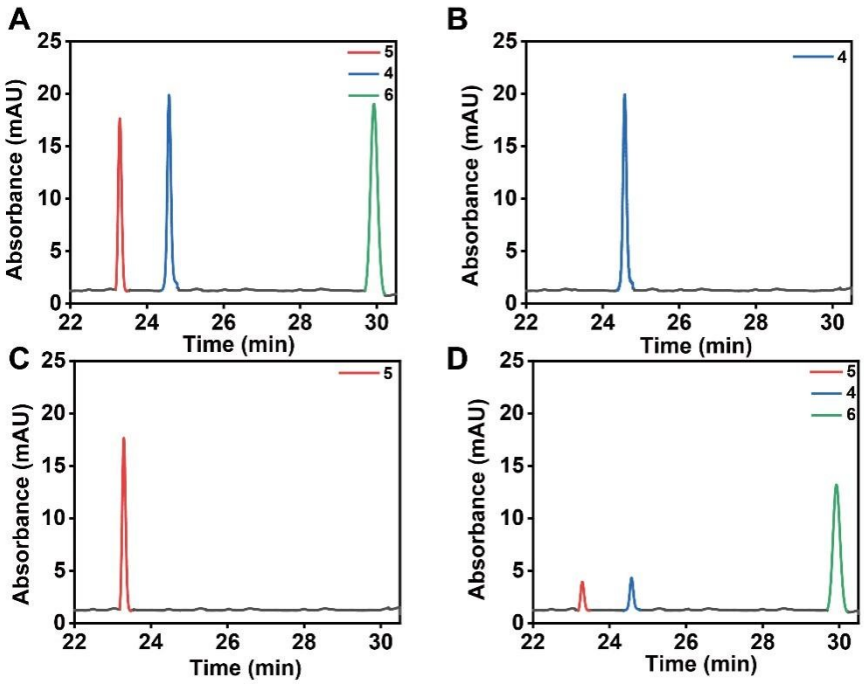

Figure S27. HPLC analysis of cell lysate after reaction catalyzed by D-Cu. A-C) HPLC chromatograms of the standard examples of **4**, **5**, and **6**. The retention times of **4**, **5**, and **6** were 24.6, 23.3, and 29.9 min, respectively. D) HPLC chromatogram of the cell lysate confirmed the presence of click coupling product **6**.

The analyses of HPLC conditions:

Detector: UV detector

Wavelength: 306 nm

Chromatographic column: Waters T3 C18 column (100×2.1 mm, 3 μm)

Mobile phase: A: 0.005 mol/L Ammonium acetate solution; B: Acetonitrile (gradient elution)

Flow rate: 0.2 ml/min

Injection volume: 10 μL

Column temperature: 25 ℃

Table. The analyses of HPLC conditions

Time（min）	A phase concentration（%）	B phase concentration（%）
0	5	95
3	5	95
13	50	50
18	95	5
23	95	5
27	5	95
30	5	95

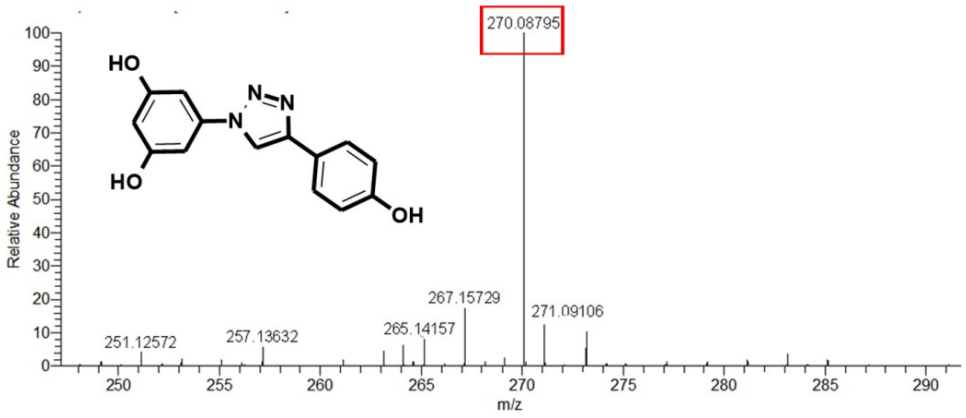

Figure S28. The LC-MS analysis of the cell lysate confirmed the presence of click coupling product **6**.

Supplementary 6. Targeted prodrug activation *in vivo* for Tumor Therapy

***Caenorhabditis elegans* (*C. elegans*) experiments.** Wild-type (N2) strain were cultured in nematode growth medium (NGM) containing *E. coli* (OP50) at 20℃. D-Cu (5 μM) was incubated with the N2 worms (about 50 worms per plate) for worm paralysis assay. After 4 h, worms were washed with PBS for 3 times to remove excess D-Cu. Next, azide coumarin **1** (10 μM) and alkyne **2** (10 μM) were added， and incubated for 12 h. Worms were washed with PBS twice and fixed with 4% paraformaldehyde. The images of worms were taken using a fluorescence microscope after being washed by PBS.

Athymic nude mouse experiments

Healthy six-week-old *BalB/c nude mice* (14~16 g) were purchased from Laboratory Animal Center of Jilin University (Changchun, China). They were housed in a specific pathogen-free environment at 26±1 ℃ and 50±5% humidity, with a 12h light-dark cycle. The handling procedures of animal were in accordance with the guidelines of the Animal Ethics Committee of Jilin University for Animal Experiments.

The biocompatibility of D-Cu in athymic nude mouse.

Hemolysis test of D-Cu was first carried out. 1 mL whole blood was collected in tubes containing Li-heparin from the Orbital venous of *BalB/c-nu* mice. Then, 1 mL blood was mixed with proper amount of 1×PBS and centrifuged for 5 min at 1118 g. The supernatant was removed. Repeat 3-4 times until the supernatant became colorless and transparent. The precipitated erythrocytes were dispersed in 1×PBS to get erythrocyte suspension. The erythrocyte suspension diluted with ultrapure water was placed in tube 1 as positive control. The erythrocyte suspension diluted with 1×PBS was placed in tube 2 as negative control. In tube 3-7, D-Cu with final concentrations of 3.125, 6.25, 12.5, 25, 50 μM were added to the erythrocyte suspension (from left to

right). These tubes were incubated for 8 h at room temperature. The hemolysis phenomena were observed and recorded. The specific absorption of hemoglobin at 540 nm was recorded and analyzed. The hemolysis rate (HR %) was calculated according to the following equation:

$$HR\% = (A_{D\text{-}Cu} - A_{NC}) \times 100\% / (A_{PC} - A_{NC}) \quad (1)$$

where $A_{D\text{-}Cu}$, A_{PC} and A_{NC} are the absorbance of the sample, the positive control, and the negative control, respectively.

Healthy BalB/c-nu mice were randomly divided into two groups. The mice in control group and experimental group were intravenously injected with PBS and D-Cu (3.5 mg kg^{-1}), respectively. Blood samples of the mice at different periods were collected for whole blood panel analysis and serum biochemical analysis. The blood biochemistry markers (WBC, RBC, MCV, HCT, MCH, MCHC, PLT and HGB), liver function markers (ALT, ALP, ALB, AST, and TP) and kidney function markers (BUN and CREA) were tests. Within 28 days after injection, the weight of mice was measured every 3 days. On the 28^{th} day, the heart, liver, spleen, lung, and kidney of mice were collected, and fixed with 4% paraformaldehyde for subsequent H&E staining.

Biodistribution and pharmacokinetics of the nanocatalyst in tumor-bearing mice. The mice were intravenously injected with D-Cu (3.5 mg kg^{-1}). At 4, 12 and 24 hours after injection, the mice were sacrificed. The organs and tumors were collected and digested in aqua regia at 80°C. The accurate distribution was evaluated by ICP-MS.

Targeted prodrug activation of D-Cu in CuAAC reaction for cancer therapy *in vivo*.

The HeLa tumor-bearing mice were divided into seven groups and treated under different conditions: (1) control; (2) G-Cu; (3) D-Cu; (4) **4**+**5**; (5) **4**+**5**+WA-Cu; (6) **4**+**5**+G-Cu;(7) **4**+**5**+ D-Cu. The mice were intravenously injected with D-Cu or G-Cu

or WA-Cu (3.5 mg kg^{-1}), respectively. After 4 hours, prodrugs **4** and **5** (20 mg kg^{-1}) were administered intraperitoneally. PBS was used as the control.

H&E staining. The major organs (heart, liver, spleen, lung, and kidney) of the mice in the above seven groups were collected, and fixed with neutral buffered formalin (10%). Then the organs were embedded into paraffin and sectioned into 4 μm thickness for H&E staining. Furthermore, to evaluate the pathological damages to tumors, the tumor tissues sections were collected for H&E staining. The images of these sections were taken using microscope under bright field.

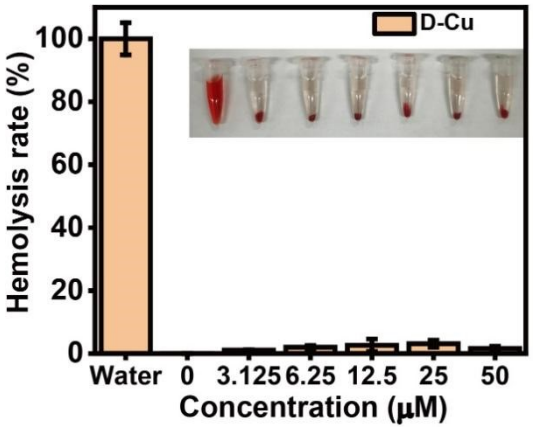

Figure S29. Hemolysis rate (HR%) of D-Cu and photograph of hemolysis test (insert). Data were presented as mean ± SD.

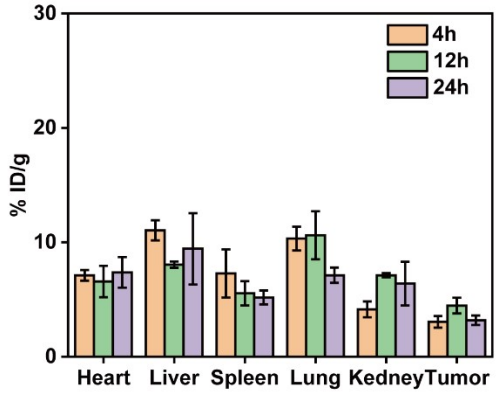

Figure S30. The biodistribution of catalyst in HeLa tumor-bearing mice at different time points using ICP-MS analysis. Data were presented as mean ± SD (n = 3 independent experiments).

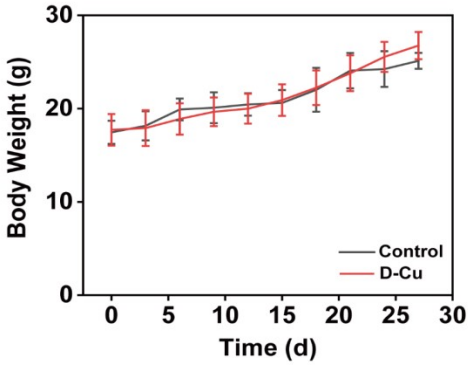

Figure S31. Body weights of mice treated with PBS or D-Cu, recorded every three days. Data were presented as mean ± SD (n = 4 independent experiments).

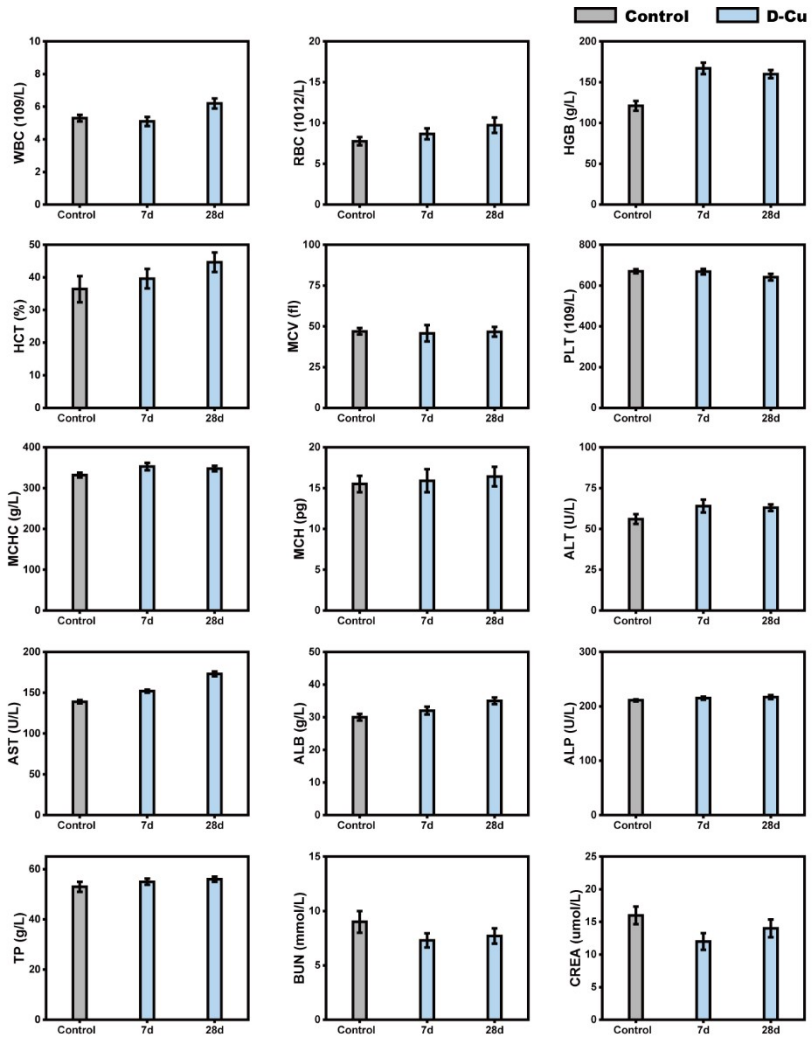

Figure S32. The hematological parameters and blood biochemical levels of the mice after injection of PBS or D-Cu collected on 7, 28 days post injection. Data were presented as mean ± SD (n = 3 independent experiments).

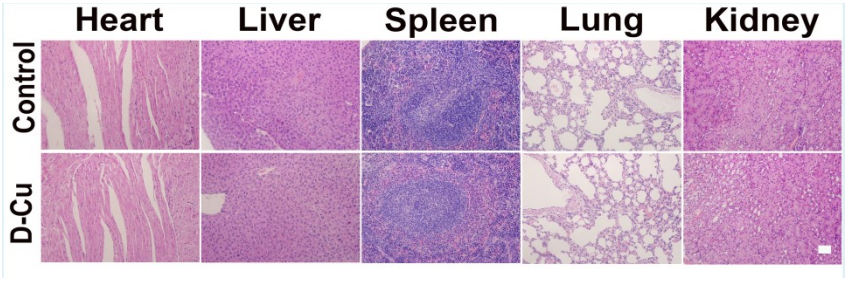

Figure S33. H&E stained images of major organs 28 days after the injection of D-Cu. No abnormalities were observed in major organs compared with those of control group. Images are representative of three independent biological samples. (Scale bar= 50 μm)

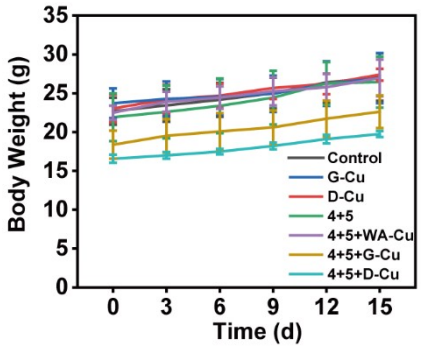

Figure S34. Changes of body weight of the mice in each group treated with different conditions. Data were presented as mean ± SD (n = 5).

Supplementary 7. Synthesis of Chemical Substrate Molecules

3-Azido-7-hydroxy-chromen-2-one (3-Azido-7-hydroxycoumarin) (1)

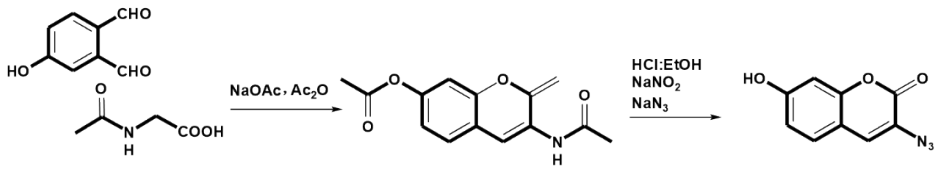

N-acetylglycine (20 mmol), 2, 4-dihydroxybenzaldehyde (20 mmol), anhydrous sodium acetate (60 mmol) were dissolved in 100 ml of acetic anhydride. Then the mixture refluxed under magnetic stirring. After 4 h, the mixture was put on the ice to obtain the yellow solid. The resulting solid was gathered using filtration and washed by ice water before it was refluxed in a solution of conc. HCl and CH_2OH (2:1) for 1 h. Then 40 mL ice water and $NaNO_2$ (40 mmol) were sequentially added into the solution in an ice bath. After stirring about 5 minutes, NaN_3 (60 mmol) was added in portions. After 15 minutes, the product was separated by filtration, washed with ultrapure water, and dried to obtain a brown solid; the yield was about 54 %. The product was pure enough for further reactions.[10] ^{1}H NMR and ^{13}C NMR (600 MHz, DMSO-*d*6).

^{1}H NMR (600 MHz, DMSO-*d*6) δ 10.53 (s, 1H), 7.61 (s, 1H), 7.50 (d, J = 8.5 Hz, 1H), 6.81-6.84 (dd, J= 8.5, 2.2 Hz, 1H), 6. 77 (d, J = 2.1 Hz, 1H).

^{13}C NMR (600 MHz, DMSO-*d*6) δ 159.8, 156.9, 152.6, 128.6, 127.4, 120.7, 110.8, 101.5.

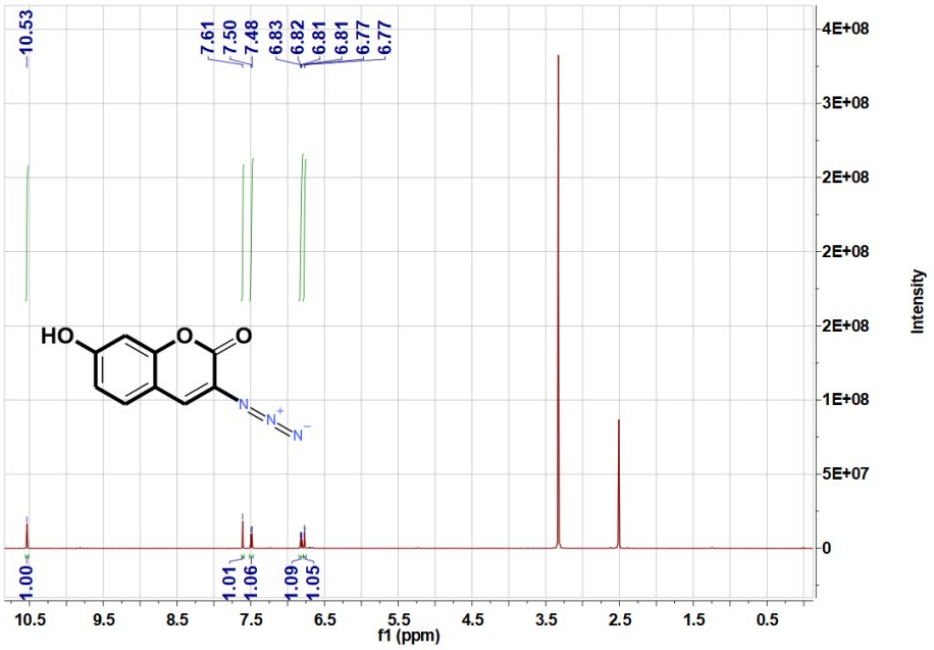

Figure S35. ^{1}H NMR spectrum of 3-Azido-7-hydroxy-chromen-2-one (3-Azido-7-hydroxycoumarin), **1**. (H_2O δ=3.3; DMSO-*d6* δ=2.5).

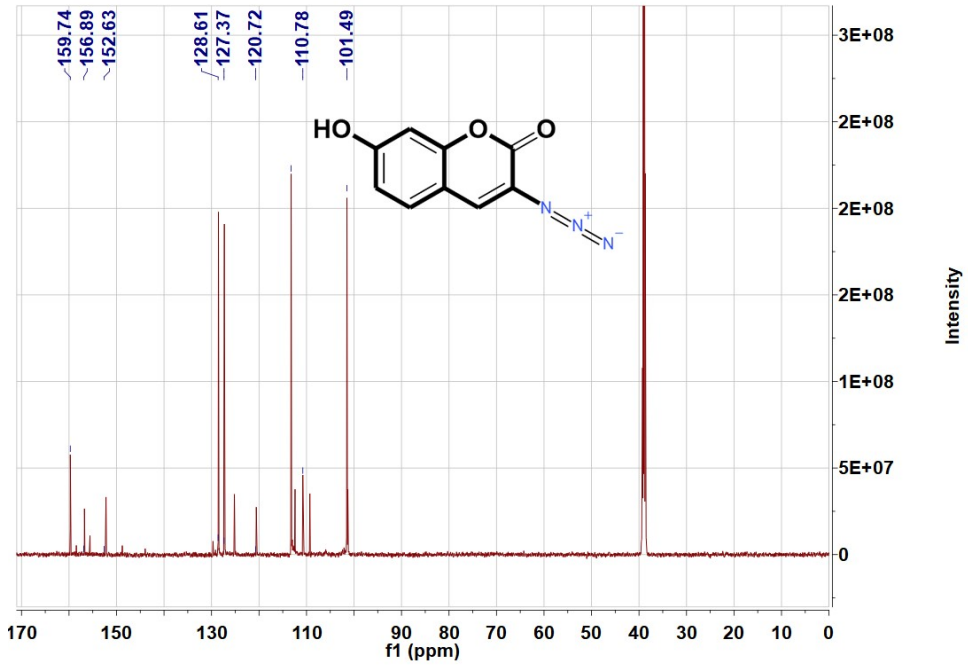

Figure S36. ^{13}C NMR spectrum of 3-Azido-7-hydroxy-chromen-2-one (3-Azido-7-hydroxycoumarin), **1**. (DMSO-*d6* δ=38.5).

7-hydroxy-3-(4-phenyl-1H-[1,2,3]triazole-1-yl)-coumarin (3)

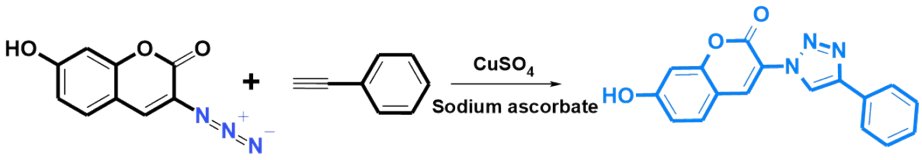

In a mixture of phenylacetylene (18 mg, 0.17 mmol) and 3-Azido-7-hydroxycoumarin(35.6 mg, 0.17 mmol) in water and ethyl alcohol (v/v = 1:1, 5 mL), sodium ascorbate (34 µL, 0.034 mmol) of freshly prepared 1 M aqueous solution was added, followed by the addition of 7.5 % copper (II) sulfate pentahydrate (28 µL, 0.0085 mmol). The heterogeneous mixture was stirred vigorously overnight in the dark at room temperature. After 10 h, the ethanol was removed and the residue was diluted with water (5 mL), cooled in ice. Then the precipitate was collected by filtration. After washing the precipitate with cold water (10 ml), the crude material was purified *via* silica gel column chromatography using CH_2Cl_2: MeOH (95:5) as the eluent, and was dried under vacuum to afford pure product as a brown powder (65%).

^{1}H NMR and ^{13}C NMR (600 MHz, DMSO-*d*6).

^{1}H NMR (600 MHz, DMSO-*d*6) δ 10.94 (s, 1H), 9.01 (s, 1H), 8.67 (s, 1H), 7.96 (s, 2H), 7.50(s, 1H), 7.39 (s, 2H), 7.38 (s, 1H), 6.93 (s, 1H), 6.89 (s, 1H)

^{13}C NMR (600 MHz, DMSO-*d*6) δ 162.0, 155.9, 154.3, 145.9, 136.3, 130.5, 129.6, 128.5, 127.7, 124.9, 118.8, 113.9, 101.7.

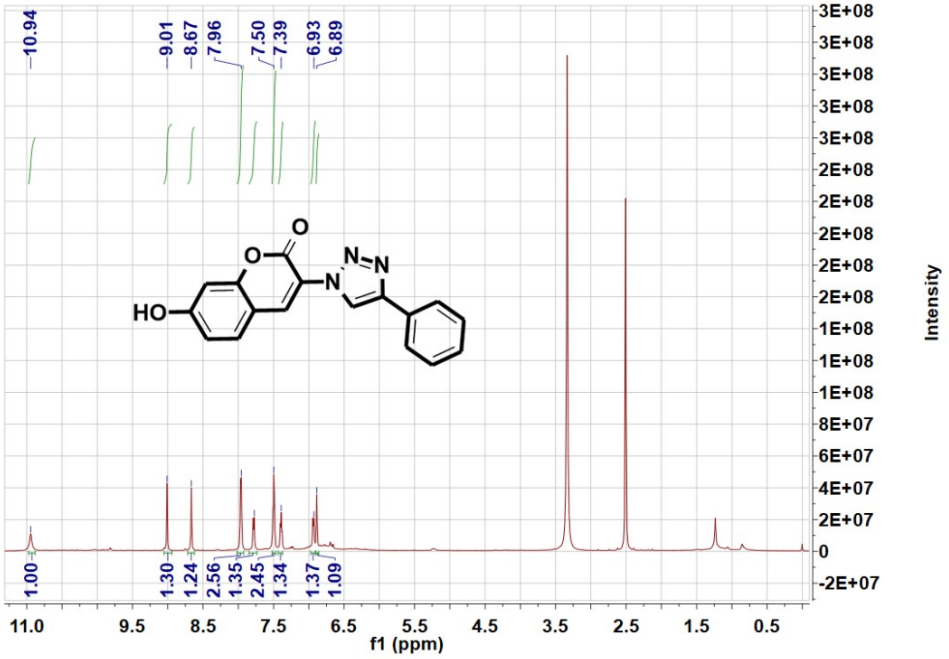

Figure S37. ^{1}H NMR spectrum of 7-hydroxy-3-(4-phenyl-1H-[1, 2, 3] triazole-1-yl)-coumarin, **3**. (H_2O δ=3.3; DMSO-*d6* δ=2.5).

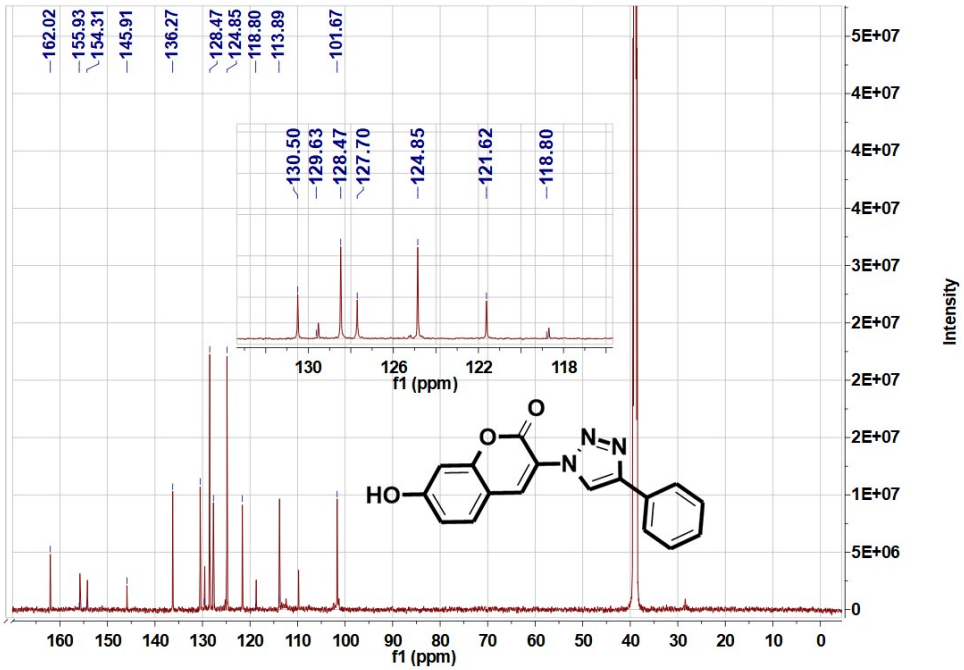

Figure S38. ^{13}C NMR spectrum of 7-hydroxy-3-(4-phenyl-1H-[1, 2, 3] triazole-1-yl)-coumarin, **3**. (DMSO-*d6* δ=38.5).

4-ethynylphenol (4)

Ethynyltrimethylsilane (6.72 mmol) was added to a solution of 4-iodophenol (4.64 mmol), Pd $(PPh_3)_2Cl_2$ (0.140 mmol) and CuI (0.140 mmol) in 15 mL Et_3N and the mixture was refluxed at 80 °C for 3 h under nitrogen. The solution was then cooled to room temperature, filtered, concentrated in vacuo and the crude product was chromatographed with Hexane/EtOAc as eluant, to obtain the precursor of compound (**5**), trimethylsilyl ethynyl phenol (880 mg, 4.62 mmol, quantitative) as the brown oil. 2 mL Aqueous NaOH (5 M) was added to a solution of 4-((trimethylsilyl)ethynyl)phenol (2.74 mmol) in 10 mL MeOH and the reaction solution was stirred for 3 h at room temperature under nitrogen. Then the solution was neutralized with conc. HCl and extracted with DCM (3 x 20 mL). The organic layers were combined, washed with brine (1 x 20 mL), dried over anhydrous $MgSO_4$, and concentrated under vacuum. The crude product was chromatographed with Hexane/EtOAc as eluant, to afford the ethynylphenol (the yield was about 58 %) as a dark red solid.[12] ^1H NMR and ^{13}C NMR (600 MHz, $CDCl_3$).

^1H NMR (600 MHz, $CDCl_3$): δ 7.92 (d, J = 8.7 Hz, 2H), 6. 9 (d, J = 8.7 Hz, 2H), 4.94 (br, 1H), 3.00 (s, 1H).

^{13}C NMR (600 MHz, $CDCl_3$) δ 155.9, 129.9, 127.4, 114.9, 114.6.

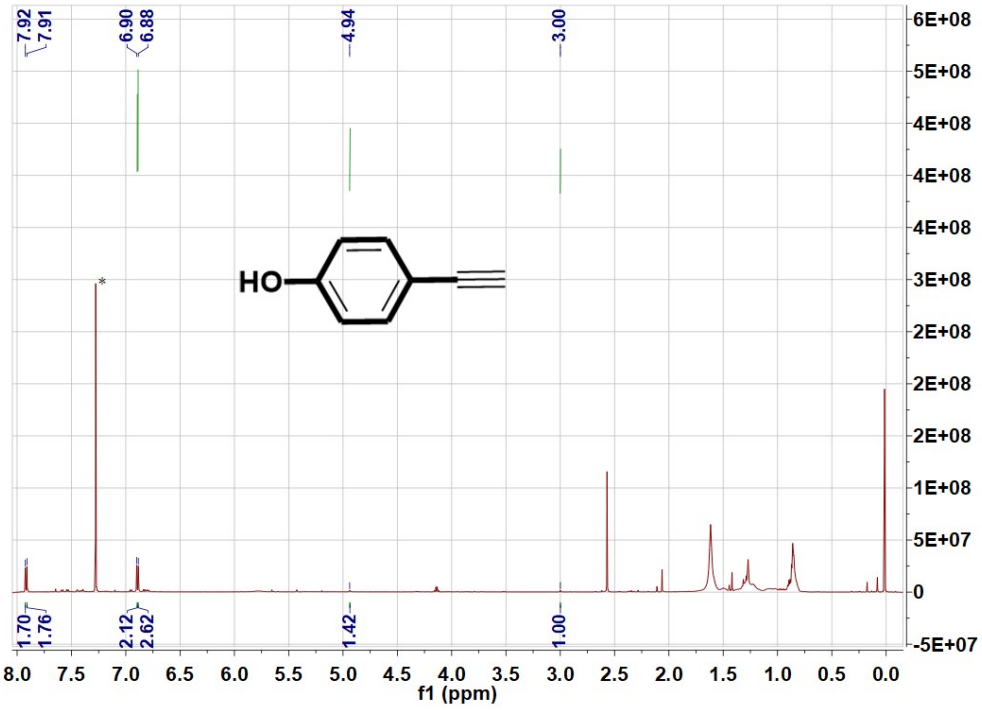

Figure S39. ^{1}H NMR spectrum of 4-ethynylphenol, **4**. (*d*-$CDCl_3$; δ=7.26).

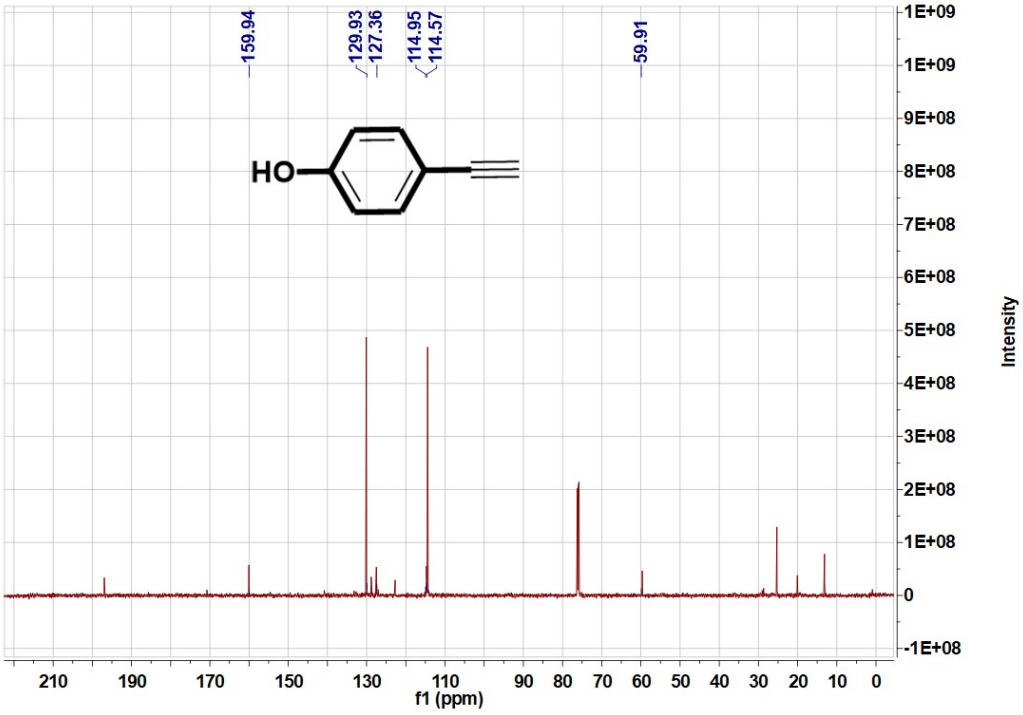

Figure S40. ^{13}C NMR spectrum of 4-ethynylphenol, **4**. (*d*-$CDCl_3$; δ=76).

5-azidobenzene-1,3-diol (5)

Phloroglucinol (79.5 mmol) and 78 mL $NH_3 \cdot H_2O$ were mixed under N_2 atmosphere. The mixture was stirred for 24h, then the solution was distilled in vacuum to remove the solvent. HCl (6 M) was added under ice bath to product the hydrochloric acid salt. The solvent distilled in vacuum, and then the product was purified through MeOH/CH_2Cl_2 reprecipitation. The obtained yellow precipitation is the precursor of compound (**5**).[11]

5 g of 5-Aminoresorcinol hydrochloride was added to a solution of 12.5 mL distilled water and 12.5 mL conc. HCl at 0 °C. $NaNO_2$ (28 mmol) dissolved in 12.5 mL distilled water was added to the above solution slowly (>5 min). After 10 min, NaN_3 (33 mmol) dissolved in 12.5 mL distilled water was added, and the reaction then allowed to stir for additional 40 min at 0 °C. The resulting solution was extracted with EtOAc (3 x 20 mL). Organic layers were combined, washed with brine (1 x 20 mL), dried over anhydrous $MgSO_4$, and concentrated under vacuum. The crude product was chromatographed with Hexane/EtOAc as eluant, to afford the light-yellow crystal, **5**. ^{1}H NMR and ^{13}C NMR (600 MHz).

^{1}H NMR (600 MHz, d-acetone) δ 8.58 (s, 1H), 6.20 (s, 1H), 6.08 (d, J = 2.1 Hz, 1H).

^{13}C NMR (600 MHz, DMSO) δ 141, 127, 122, 115.

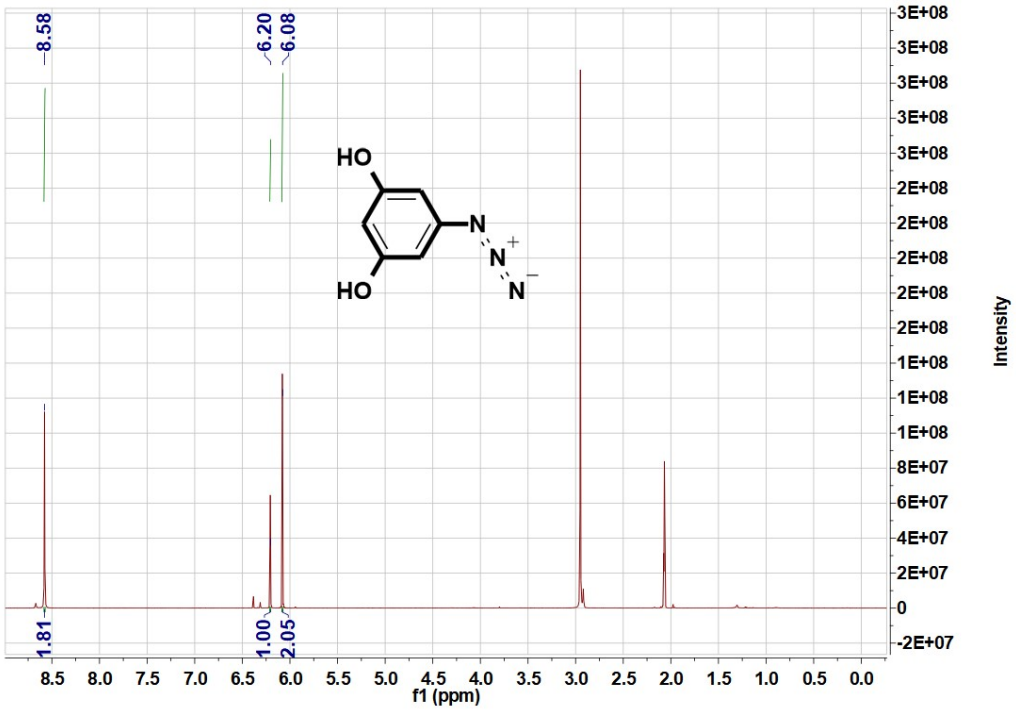

Figure S41. [1]HNMR spectrum of 5-azidobenzene-1, 3-diol, **5** (H_2O δ=3.3; *d*-acetone δ=2.05).

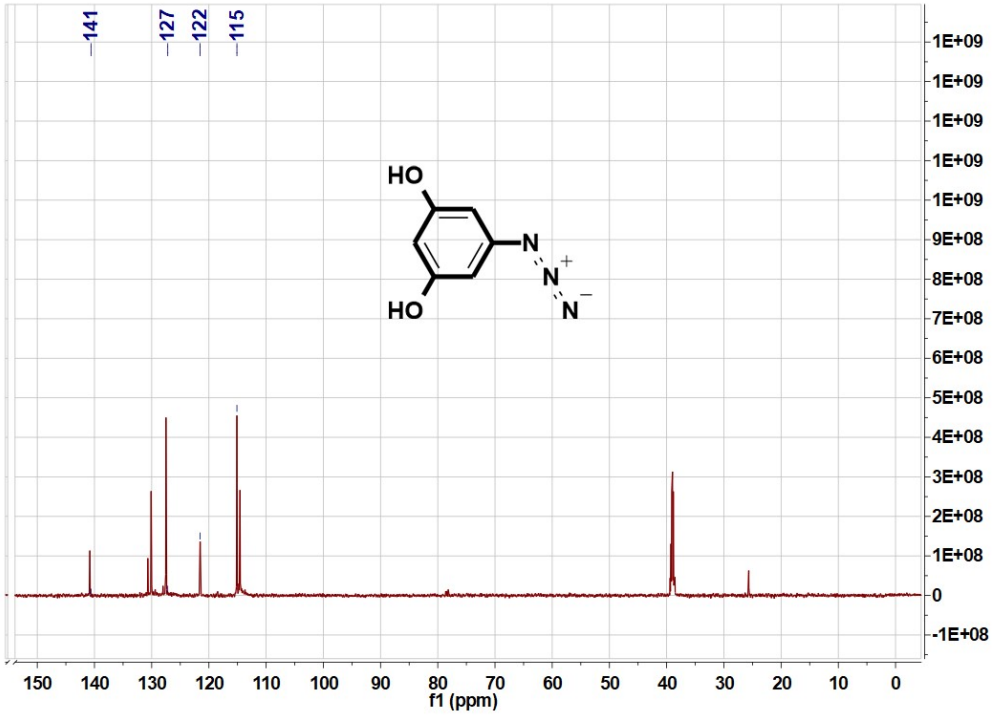

Figure S42. [13]CNMR spectrum of 5-azidobenzene-1, 3-diol, **5** (DMSO-*d6* δ=38.5).

5-(4-(4-hydroxyphenyl)-1H-1,2,3-triazol-1-yl)benzene-1,3-diol (6)

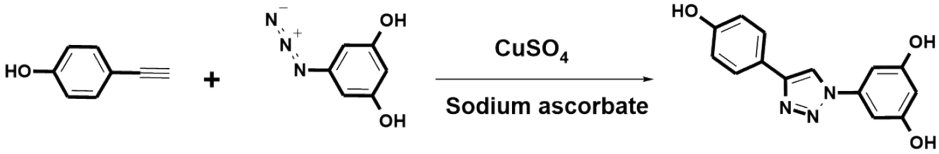

The synthesis was carried out with the following conditions: the overall volume in each test tube was 2 mL (H_2O: t-ButOH=1:1), containing a solution of alkyne, **4**, (1 eq) and azide, **5**, (1 eq). Sodium ascorbate (0.5 eq) of freshly prepared solution in water was added, followed by the addition of copper (II) sulfate pentahydrate (0.05 eq). The resulting reaction was vigorously stirred for 6 h at 25°C. The reaction mixture was then diluted with water, cooled in ice, and the precipitate was collected by filtration. After washing the precipitate with diethyl ether, it was dried under vacuum to afford a solid. ^{1}H NMR and ^{13}C NMR (600 MHz, DMSO-*d*6).

^{1}H NMR (600 MHz, DMSO-*d*6) δ 9.67 (s, 1H), 9.58 (s, 1H), 9.56 (s, 1H), 7.96 (s, 1H), 7.64 (d, J = 8.5 Hz, 2H), 6.89 (d, J = 8.5 Hz, 1H), 6.71 (d, J = 8.5 Hz, 1H), 6.04 (d, J = 1.9 Hz, 2H), 5.94 (s, 1H).

^{13}C NMR (600 MHz, DMSO-*d*6) δ 160.08, 152.21, 128.54, 127.30, 125.18, 113.24, 112.41, 110.69, 101.30.

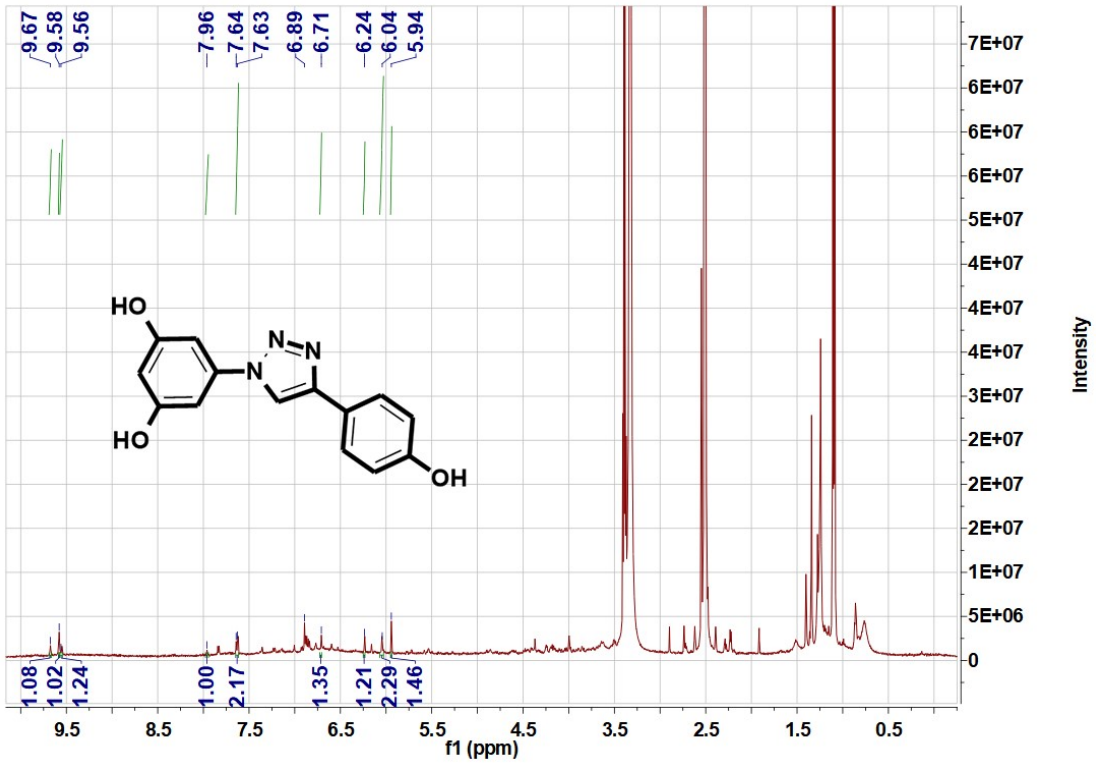

Figure S43. ^{1}H NMR spectrum of 5-(4-(4-hydroxyphenyl)-1H-1,2,3-triazol-1-yl)benzene-1,3-diol, **6**. (H_2O δ=3.3; *d*-DMSO δ=2.5)

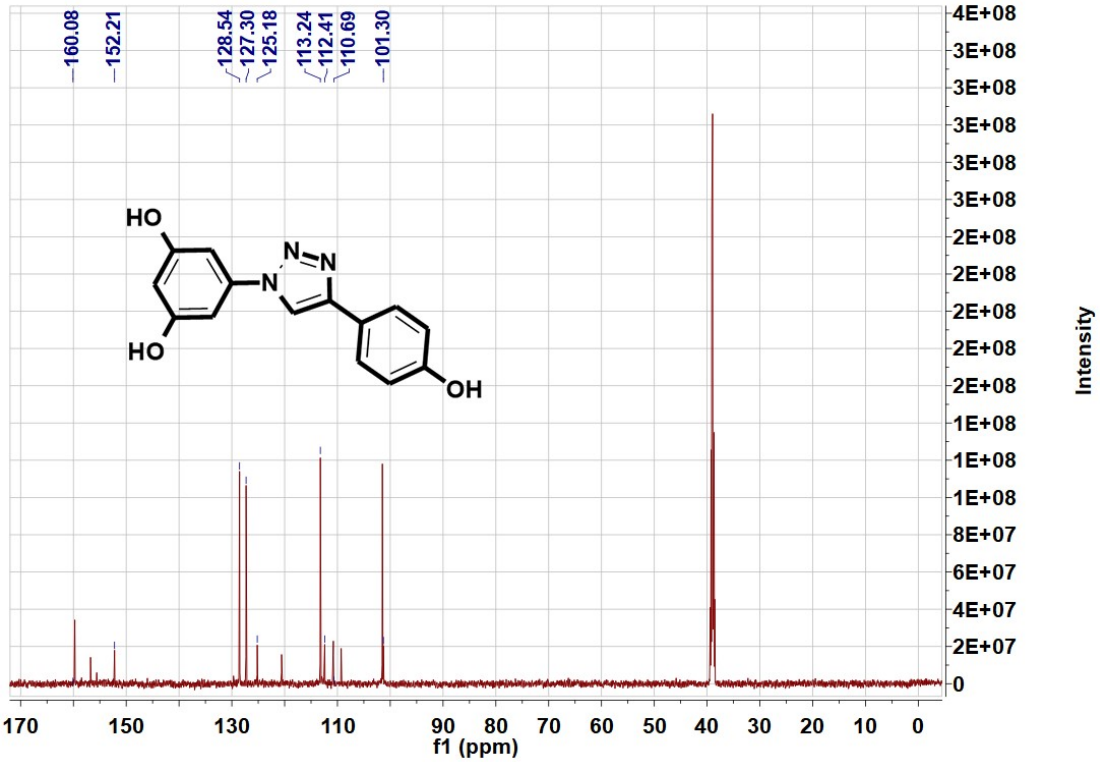

Figure S44. ^{13}C NMR spectrum of 5-(4-(4-hydroxyphenyl)-1H-1,2,3-triazol-1-yl)benzene-1,3-diol, **6**. (*d*-DMSO δ=38.5)

References

1.Reuter, J. S.; Mathews, D. H., RNAstructure: software for RNA secondary structure prediction and analysis. Bmc Bioinformatics 2010, 11.

2.Phillips, J. C.; Braun, R.; Wang, W.; Gumbart, J.; Tajkhorshid, E.; Villa, E.; Chipot, C.; Skeel, R. D.; Kale, L.; Schulten, K., Scalable molecular dynamics with NAMD. J. Comput. Chem. 2005, 26 (16), 1781-802.

3.Best, R. B.; Zhu, X.; Shim, J.; Lopes, P. E.; Mittal, J.; Feig, M.; Mackerell, A. D., Jr., Optimization of the additive CHARMM all-atom protein force field targeting improved sampling of the backbone phi, psi and side-chain chi(1) and chi(2) dihedral angles. J. Chem. Theory. Comput. 2012, 8 (9), 3257-3273.

4.Klauda, J. B.; Venable, R. M.; Freites, J. A.; O'Connor, J. W.; Tobias, D. J.; Mondragon-Ramirez, C.; Vorobyov, I.; MacKerell, A. D., Jr.; Pastor, R. W., Update of the CHARMM all-atom additive force field for lipids: validation on six lipid types. J. Phys. Chem. B 2010, 114 (23), 7830-43.

5.Martyna, G. J.; Tobias, D. J.; Klein, M. L., Constant-Pressure Molecular-Dynamics Algorithms. J. Chem. Phys. 1994, 101 (5), 4177-4189.

6.Feller, S. E.; Zhang, Y. H.; Pastor, R. W.; Brooks, B. R., Constant-Pressure Molecular-Dynamics Simulation - the Langevin Piston Method. J. Chem. Phys. 1995, 103 (11), 4613-4621.

7.Essmann, U.; Perera, L.; Berkowitz, M. L.; Darden, T.; Lee, H.; Pedersen, L. G., A Smooth Particle Mesh Ewald Method. J Chem Phys 1995, 103 (19), 8577-8593.

8.Trott, O.; Olson, A. J., Software News and Update AutoDock Vina: Improving the Speed and Accuracy of Docking with a New Scoring Function, Efficient Optimization, and Multithreading. J Comput Chem 2010, 31 (2), 455-461.

9.Laskowski, R. A.; Swindells, M. B., LigPlot+: Multiple Ligand-Protein Interaction Diagrams for Drug Discovery. J Chem Inf Model 2011, 51 (10), 2778-2786.

10.Sivakumar, K.; Xie, F.; Cash, B. M.; Long, S.; Barnhill, H. N.; Wang, Q. A Fluorogenic 1, 3-Dipolar Cycloaddition Reaction of 3-Azidocoumarins and Acetylenes. Org. Lett. 2004, 6, 4603-4606.

11. Andrus, M.B.; Liu, J.; Meredith, E.L.; Nartey, E., Synthesis of Resveratrol Using a Direct Decarbonylative Heck Approach from Resorcylic Acid. Tetrahedron Lett. 2003, 44, 4819-4822.

12. Hudson, S. A.; McLean, K. J.; Surade, S.; Yang, Y. Q.; Leys, D.; Ciulli, A.; Munro, A. W.; and Abell, C, Application of Fragment Screening and Merging to the Discovery of Inhibitors of the Mycobacterium Tuberculosis Cytochrome P450 CYP121. Angew. Chem. Int. Ed. 2012, 51, 9311-9316.